Patterned femtosecond-laser ablation of *Xenopus laevis* melanocytes for studies of cell migration, wound repair, and developmental processes

Jessica P. Mondia,[1,3,4] Dany S. Adams,[2,4] Ryan D. Orendorff,[1] Michael Levin,[2] and Fiorenzo G. Omenetto[1,3,*]

[1]*Department of Biomedical Engineering, Tufts University, 4 Colby Street, Medford, MA 02155, USA*
[2]*Department of Biology and Tufts Center for Regenerative and Developmental Biology, Tufts University, 200 Boston Ave., Medford, MA 02155, USA*
[3]*Department of Physics, Tufts University, 4 Colby Street, Medford MA 02155, USA*
[4]*These authors contributed equally*
**Fiorenzo.Omenetto@Tufts.edu*

Abstract: Ultrafast (femtosecond) lasers have become an important tool to investigate biological phenomena because of their ability to effect highly localized tissue removal in surgical applications. Here we describe programmable, microscale, femtosecond-laser ablation of melanocytes found on *Xenopus laevis* tadpoles, a technique that is applicable to biological studies in development, regeneration, and cancer research. We illustrate laser marking of individual melanocytes, and the drawing of patterns on melanocyte clusters to help track their migration and/or regeneration. We also demonstrate that this system can upgrade scratch tests, a technique used widely with cultured cells to study cell migration and wound healing, to the more realistic *in vivo* realm, by clearing a region of melanocytes and monitoring their return over time. In addition, we show how melanocyte ablation can be used for loss-of-function experiments by damaging neighboring tissue, using the example of abnormal tail regeneration following localized spinal cord damage. Since the size, shape, and depth of melanocytes vary as a function of tadpole age and melanocyte location (head or tail), an ablation threshold chart is given. Mechanisms of laser ablation are also discussed.

OCIS codes: (170.1020) Ablation of tissue; (140.7090) Ultrafast lasers

References and links

1. A. Vogel, J. Noack, G. Hüttman, and G. Paltauf, "Mechanisms of femtosecond laser nanosurgery of cells and tissues," Appl. Phys. B **81**(8), 1015–1047 (2005).
2. S. H. Chung and E. Mazur, "Surgical applications of femtosecond lasers," J. Biophotonics **2**(10), 557–572 (2009).
3. K. König, "Multiphoton microscopy in life sciences," J. Microsc. **200**(2), 83–104 (2000).
4. M. F. Yanik, H. Cinar, H. N. Cinar, A. D. Chisholm, Y. Jin, and A. Ben-Yakar, "Neurosurgery: functional regeneration after laser axotomy," Nature **432**(7019), 822 (2004).
5. V. Kohli and A. Y. Elezzabi, "Laser surgery of zebrafish (*Danio rerio*) embryos using femtosecond laser pulses: optimal parameters for exogenous material delivery, and the laser's effect on short- and long-term development," BMC Biotechnol. **8**(1), 7 (2008).
6. W. Supatto, D. Débarre, B. Moulia, E. Brouzés, J.-L. Martin, E. Farge, and E. Beaurepaire, "*In vivo* modulation of morphogenetic movements in *Drosophila* embryos with femtosecond laser pulses," Proc. Natl. Acad. Sci. U.S.A. **102**(4), 1047–1052 (2005).
7. J. Green, "Morphogen gradients, positional information, and *Xenopus*: interplay of theory and experiment," Dev. Dyn. **225**(4), 392–408 (2002).
8. C. W. Beck and J. M. Slack, "An amphibian with ambition: a new role for *Xenopus* in the 21st century," Genome Biol. **2**(10), reviews1029.1–reviews1029.5 (2001).
9. J. B. Wallingford, "Tumors in tadpoles: the *Xenopus* embryo as a model system for the study of tumorigenesis," Trends Genet. **15**(10), 385–388 (1999).
10. A. S. Tseng and M. Levin, "Tail regeneration in *Xenopus laevis* as a model for understanding tissue repair," J. Dent. Res. **87**(9), 806–816 (2008).

#148794 - $15.00 USD Received 7 Jun 2011; revised 24 Jul 2011; accepted 24 Jul 2011; published 27 Jul 2011

11. J. M. W. Slack, C. W. Beck, C. Gargioli, and B. Christen, "Cellular and molecular mechanisms of regeneration in *Xenopus*," Philos. Trans. R. Soc. Lond. B Biol. Sci. **359**(1445), 745–751 (2004).
12. C. W. Beck, J. C. Izpisúa Belmonte, and B. Christen, "Beyond early development: *Xenopus* as an emerging model for the study of regenerative mechanisms," Dev. Dyn. **238**(6), 1226–1248 (2009).
13. S. L. Klein, R. L. Strausberg, L. Wagner, J. Pontius, S. W. Clifton, and P. Richardson, "Genetic and genomic tools for *Xenopus* research: The NIH *Xenopus* initiative," Dev. Dyn. **225**(4), 384–391 (2002).
14. D. S. Adams, "A new tool for tissue engineers: ions as regulators of morphogenesis during development and regeneration," Tissue Eng. Part A **14**(9), 1461–1468 (2008).
15. H. Ogino and H. Ochi, "Resources and transgenesis techniques for functional genomics in *Xenopus*," Dev. Growth Differ. **51**(4), 387–401 (2009).
16. M. L. Tomlinson, P. Guan, R. J. Morris, M. D. Fidock, M. Rejzek, C. Garcia-Morales, R. A. Field, and G. N. Wheeler, "A chemical genomic approach identifies matrix metalloproteinases as playing an essential and specific role in *Xenopus* melanophore migration," Chem. Biol. **16**(1), 93–104 (2009).
17. D. Blackiston, D. S. Adams, J. M. Lemire, M. Lobikin, and M. Levin, "Transmembrane potential of GlyCl-expressing instructor cells induces a neoplastic-like conversion of melanocytes via a serotonergic pathway," Dis Model Mech **4**(1), 67–85 (2011).
18. T. O'Reilly-Pol and S. L. Johnson, "Melanocyte regeneration reveals mechanisms of adult stem cell regulation," Semin. Cell Dev. Biol. **20**(1), 117–124 (2009).
19. P. D. Nieuwkoop and J. Faber, *Normal Table of Xenopus laevis (Daudin): a Systematical and Chronological Survey of the Development from the Fertilized Egg Till the End of Metamorphosis* (North-Holland, Amsterdam, 1956).
20. M. Kumasaka, H. Sato, S. Sato, I. Yajima, and H. Yamamoto, "Isolation and developmental expression of Mitf in *Xenopus laevis*," Dev. Dyn. **230**(1), 107–113 (2004).
21. C.-T. Yang, R. D. Sengelmann, and S. L. Johnson, "Larval melanocyte regeneration following laser ablation in zebrafish," J. Invest. Dermatol. **123**(5), 924–929 (2004).
22. H. L. Sive, R. M. Grainger, and R. M. Harland, *Early Development of Xenopus laevis: a Laboratory Manual* (Cold Spring Harbor Laboratory Press Cold Spring Harbor, NY, 2000).
23. J. Morokuma, D. Blackiston, D. S. Adams, G. Seebohm, B. Trimmer, and M. Levin, "Modulation of potassium channel function confers a hyperproliferative invasive phenotype on embryonic stem cells," Proc. Natl. Acad. Sci. U.S.A. **105**(43), 16608–16613 (2008).
24. R. M. Steinman, "An electron microscopic study of ciliogenesis in developing epidermis and trachea in the embryo of *Xenopus laevis*," Am. J. Anat. **122**(1), 19–55 (1968).
25. Z. B. Wang, M. H. Hong, Y. F. Lu, D. J. Wu, B. Lan, and T. C. Chong, "Femtosecond laser ablation of polytetrafluoroethylene (Teflon) in ambient air," J. Appl. Phys. **93**(10), 6375–6380 (2003).
26. T. H. Morgan, *Regeneration* (The Macmillan Company, 1901).
27. J. M. Slack, G. Lin, and Y. Chen, "Molecular and cellular basis of regeneration and tissue repair: the *Xenopus* tadpole: a new model for regeneration research," Cell. Mol. Life Sci. **65**(1), 54–63 (2008).
28. Y. Taniguchi, T. Sugiura, A. Tazaki, K. Watanabe, and M. Mochii, "Spinal cord is required for proper regeneration of the tail in *Xenopus* tadpoles," Dev. Growth Differ. **50**(2), 109–120 (2008).
29. J. P. Mondia, M. Levin, F. G. Omenetto, R. D. Orendorff, and D. S. Adams, "Long-distance positional signals are required for normal morphogenesis during regeneration of the *Xenopus* tadpole tail, as revealed by femtosecond-laser cell ablation along the dorsal axis," in preparation.
30. K. Kuetemeyer, R. Rezgui, H. Lubatschowski, and A. Heisterkamp, "Influence of laser parameters and staining on femtosecond laser-based intracellular nanosurgery," Biomed. Opt. Express **1**(2), 587–597 (2010).
31. A. M. Burgoyne, J. M. Palomo, P. J. Phillips-Mason, S. M. Burden-Gulley, D. L. Major, A. Zaremba, S. Robinson, A. E. Sloan, M. A. Vogelbaum, R. H. Miller, and S. M. Brady-Kalnay, "PTPμ suppresses glioma cell migration and dispersal," Neuro-oncol. **11**(6), 767–778 (2009).

1. Introduction

Femtosecond (fs) Ti:sapphire lasers have been used to investigate biological phenomena in many different types of organisms, particularly for submicron laser ablation studies [1,2]. By operating the Ti:sapphire laser around 800 nm, away from the absorption of most tissues [3], and capitalizing on the short duration of the laser pulses, ablation can occur at less than the laser beam's focal volume while offering deeper tissue penetration. In the field of developmental biology, fs-lasers have been used to sever the nerve axons of worms [4], to study short- and long-term development after laser ablation of zebrafish cells [5], and to dissect drosophila embryos for the study of morphogenetic movements [6].

Effects of laser surgery on embryos of *Xenopus laevis* (the African clawed frog) are as yet unexplored. This constitutes a valuable opportunity given the importance of this amphibian as a well-studied model of vertebrate development [7,8], cancer [9], and regeneration [10–12]. *Xenopus* are widely used in developmental biology because their embryos are readily raised in laboratory culture, accessible from the earliest stages and throughout organogenesis, relatively quick to develop, large and easy to manipulate, and highly resistant to infection. Also, the

#148794 - $15.00 USD Received 7 Jun 2011; revised 24 Jul 2011; accepted 24 Jul 2011; published 27 Jul 2011

tadpoles are largely transparent. Most importantly, their development is known in detail, and the embryos are amenable to a wide range of manipulations using molecular-genetic, cell-biological, pharmacological, optical, and biophysical techniques [13–15]. For studies of cancer-like cell behavior, melanocytes, the melanin-containing cells that constitute the darkly pigmented spots in the animal's skin, can be induced to behave like neoplastic cells, making them an interesting *in vivo* model for melanoma [16,17]. Moreover, melanocytes are descendants of a vertebrate-specific stem cell population called the neural crest [18], and their study can thus shed light on many aspects of the complex signaling by which an animal integrates functions of stem cells and their descendants into the developmental programs of the host—a research topic crucial for advances in regenerative medicine and cancer biology.

In this paper, we focus on the use of ultrafast lasers as a tool to label, draw patterns on, and eliminate *Xenopus* melanocytes. We show how this methodology can be used to understand melanocyte migration and regeneration, and the relationship between tail regeneration and particular cell types using a loss-of-function approach. Since the development of *Xenopus* is sensitive to individual variations and temperature, we refer to the stage of the *Xenopus* rather than the age [19]. Our discussion will be limited to melanocyte laser ablation in embryos between stages 35 and 46 (i.e. ~2–7 days post fertilization at 22°C), since pilot studies have shown that damage at earlier developmental stages caused no definitive disruptions to development, in agreement with published results on zebrafish embryos [5]. Our target period begins just at the end of the melanization of pigmented cells in *Xenopus*, which occurs during stages 25-40 [20]: around stages 25-30, melanin is generated in melanocyte cells located around the dorsal region; during stages 30-40, the melanocytes migrate away from the dorsal midline (the developing central nervous system and vertebral column) of the tadpole; at later stages, the melanocytes are fully pigmented and remain stationary. Where previous studies only considered melanocyte death and regeneration in zebrafish [21], or laser ablation of lines for microdissections [6], we show controlled cell ablation and pigment removal on melanocytes found in the head and along the tail, at the same dorsal-ventral level as the spinal cord, and demonstrate how these methods are useful for applications in the study of wound healing, cancer, and developmental processes.

2. Materials and methods

The optical setup used for laser surgery of *Xenopus* is shown in Fig. 1a. Pulses with a center wavelength of 810 nm, repetition rate of 80 MHz, and pulse width of 120 fs were generated from a Ti:sapphire oscillator (Spectra Physics Tsunami). The average pulse power was varied between 20 mW - 1 W using a combination of neutral density filters along with a half-wave plate and polarizing beam cube. Included in the beam path was an electro-mechanical shutter (Thorlabs SH05/SC10) with an opening time $\Delta T = 0.4$ ms and a closing time $\Delta T = 0.6$ ms. Both imaging of the specimen and pulse focusing were performed through an inverted microscope (Olympus Microscopes IX71). The laser beam was typically focused with 10x (NA = 0.3) or 20x (NA = 0.5) Olympus objectives. For the experiments reported here, we found that the narrow depth of focus associated with higher NA objectives was impractical because the tadpole surface is not flat, making focusing and marking difficult. The reported fluences account for the ellipticity of the incoming laser beam and use the measured average power (P_{avg}) after the microscope objectives. Fluences were calculated by $F = 2P_{avg}/(RR\pi ab)$ where RR is the laser repetition rate and a and b define the beam ellipticity. Using a knife edge technique, the ($1/e^2$) beam radii for the 10x objective were 2.2 μm and 2.9 μm, and those for the 20x objective were 1.7 μm and 2.3 μm. The specimen was located on top of a motorized xy stage (Ludl Electronics Products Ltd. BioPrecision2 Flat-top Inverted Stage). The sample position, CCD image acquisition, and shutter duration were computer controlled. A LabVIEW interfacing program was written to allow the laser to write images in three modes: (1) raster scanning; (2) tracing basic shapes such as grids, lines, and spirals; and (3) targeting specific locations of a live image (program available from corresponding author).

#148794 - $15.00 USD Received 7 Jun 2011; revised 24 Jul 2011; accepted 24 Jul 2011; published 27 Jul 2011

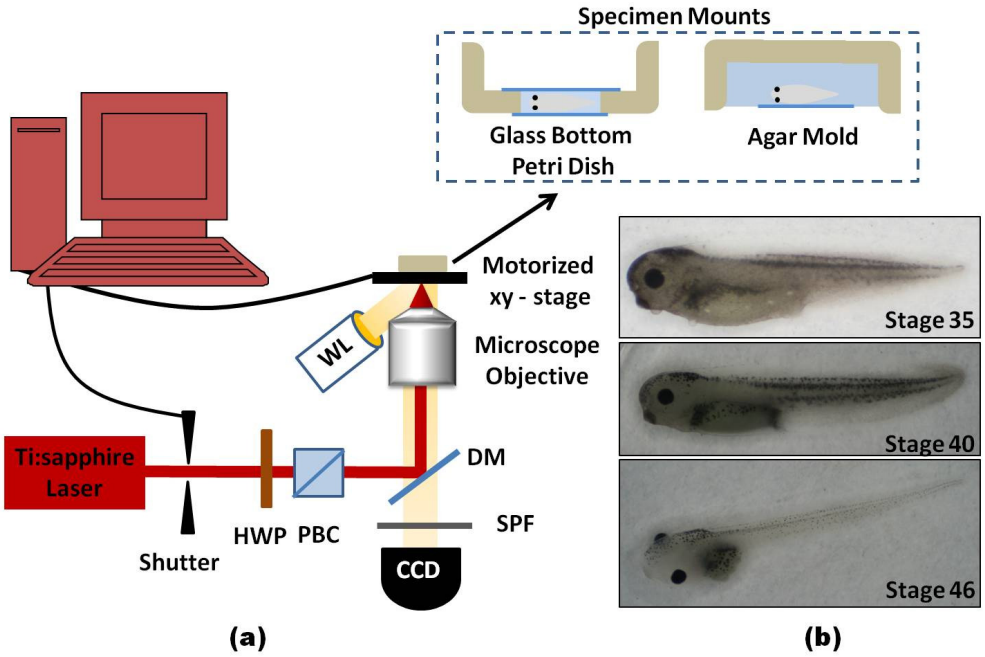

Fig. 1. Schematic of femtosecond laser ablation of *Xenopus* tadpoles. (**a**) Femtosecond pulses were focused onto the specimens mounted on top of the motorized stage. For laser ablation, *Xenopus laevis* younger than stage 40 were held between a Petri dish with a glass welled bottom and a cover slip, while older tadpoles were placed inside a depression made of agar, secured with a glass cover slip, and then inverted for placement on the stage. (HWP—half wave plate, PBC—polarizing beam cube, SPF—short pass filter, DM—dichroic mirror, WL—white light source) (**b**) Images of *Xenopus* tadpoles at three different developmental stages.

Xenopus were raised in 0.1X Marc's Modified Ringer's (MMR) solution at a temperature of 14-22°C and pH 7.8, according to standard protocols [22]. For tail amputation, tadpoles were anesthetized using 1.5% tricaine, and one third to one half of the tail was removed using a No. 10 scalpel. After five minutes, the tadpoles were returned to plain MMR. For laser ablation, stage 36-42 tadpoles were anesthetized either with 1.5% tricaine in MMR, or with 5 µL N-benzyl-p-toluene sulfonamide (BTS) in MMR for ~15 minutes prior to laser surgery. Figure 1a illustrates the two modes used to house the specimens for laser ablation. Younger tadpoles were placed into a 35 mm glass-bottomed Petri dish (WWW precision instruments) with a recessed center containing ~0.3 mL of anesthetic solution, and held in place with a square glass cover slip (22 mm x 22 mm x 0.17 mm). Older tadpoles were placed in a depression made in agar with a drop of anesthetic solution, held in place with a cover slip, and then the dish was inverted for surgery. After surgery, the tadpoles were moved into a six-well plate filled with MMR solution and maintained at 22°C for further analysis. It has been observed that size and shape of melanocytes are influenced by the anesthetic solutions (tricaine and BTS), which cause them to retract and present a smaller area to target with the laser [23]. The three stages of tadpole development we found most useful for out studies are shown in Fig. 1b.

The depth of the melanocyte relative to the surface of the tadpole was determined using DIC microscopy. With a calibrated stage, the distance was measured from focused images of ciliated cells above the melanocytes, which marked the surface, and the focused image of the melanocyte.

Time lapse movies of laser-marked migrating melanocytes were made on a Nikon AZ100m stereoscope with an attached Andor Luca-R CCD camera. The system is controlled by NIS Elements. Tadpoles were placed in depressions made in agar and contained in 35 mm

#148794 - $15.00 USD Received 7 Jun 2011; revised 24 Jul 2011; accepted 24 Jul 2011; published 27 Jul 2011

Petri dishes. The dish was then filled completely with MMR, and a large coverslip was used to seal the dish. Images were collected every 3-5 minutes.

Absorption spectra of a paste composed of ground stage 35 *Xenopus* tails and diluted in deionized water were acquired with a Varian Cary UV/VIS spectrometer.

The damage threshold was determined by focusing the laser on a specific melanocyte and delivering pulses for 10 ms duration while varying the laser fluence until a change in the pigmented tissue such as a contraction, expansion, or discoloration was observed (see Media 1). Tests were conducted at the head and tail for 2 tadpoles at stages 35, 40, and 46. Between 5 and 10 melanocytes were used at each location.

3. Results

3.1. Ablation of melanin-containing cells

Our investigations focus on the ablation of melanin-containing cells for several reasons. First, these cells are more absorptive to our laser wavelength and hence we can reduce the amount of collateral damage to the surrounding tissue. Second, melanin-containing cells are situated in several locations on the tadpole that are interesting for developmental biology, including the eye, the gut, and near the spinal cord. Lastly, these cells can be induced to show cancer-like properties. Therefore, the ability to selectively ablate such cells provides several interesting opportunities to expand our knowledge of development and neoplastic behavior.

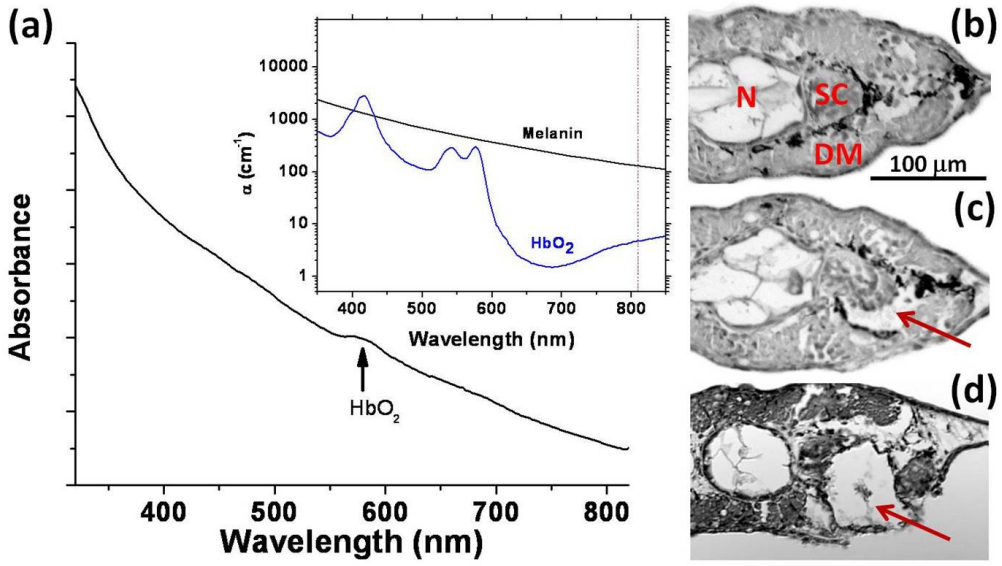

Fig. 2. (**a**) Absorption spectrum from a paste made of *Xenopus* tails and diluted in deionized water. Arrow indicates peak likely due to hemoglobin. The inset plots the absorption spectrum of melanin and oxygenated hemoglobin and the dashed line indicates the laser wavelength. (**b**) Histology section of undamaged tadpole tail (24 hpa) showing location of the notochord (N), the melanocytes surrounding the spinal cord (SC) and the dorsal muscle (DM). (**c**) Another section of the same tail where the red arrow points to absence of a melanocyte after laser treatment for one insult, i.e., shutter duration of 200ms and laser fluence of 26 mJ/cm^2. (**d**) Section showing damage to SC and DM after multiple laser insults to melanocytes.

Figure 2a is a plot of the absorption spectrum from a paste of ground *Xenopus* tails diluted in deionized water. As the wavelength increases, there is an exponential decrease in the absorption similar to melanin found in mammalian skin. The slight increase in absorption at 580 nm is likely due to oxygenated hemoglobin (HbO_2) contained in the tail paste because the major intracellular absorbers for the visible wavelength range are hemoglobin and melanin [3].

#148794 - $15.00 USD Received 7 Jun 2011; revised 24 Jul 2011; accepted 24 Jul 2011; published 27 Jul 2011

If the 810 nm laser beam is scanned along the surface of the tadpoles, at any age, we find no visible damage to the transparent regions of the tadpole for our maximum fluence of 130 mJ/cm^2. In contrast, scanning over melanocytes does produce damage depending on the number of pulses hitting the sample (i.e., shutter opening time) and the fluence used. For example, Fig. 2b and 2c are histology sections of an untreated and a laser-treated region, respectively, and illustrate that the melanocytes inside the tissue can be damaged without damaging the outer layer. Higher energies (fluence × shutter opening time) will cause greater collateral damage around the melanocyte (Fig. 2c).

Ablation of melanin-containing cells is affected by the amount of cell pigmentation and the thickness of the epidermis above the melanocytes, which varies as a function of age and location (head or tail) on the tadpole [20,24]. Table 1 highlights some of these differences. As the tadpole develops from stage 35-46, the melanocytes migrate closer to the surface and become fully pigmented. Surface melanocytes, which are <30 μm from the surface, such as those found in the head and in the tail for stage 46 *Xenopus* tadpoles, have lower damage thresholds (~3 mJ/cm^2). In contrast, melanocytes in the tail of tadpoles ranging from stages 35 to 40 have larger damage thresholds (4.8–13.6 J/cm^2) due to partially pigmented cells and to the varying melanocyte depths as they migrate to their final destination. By operating the laser near the damage threshold, we are able to mark melanocytes, and by exceeding the damage threshold, destroy melanocytes.

Table 1. Damage threshold for *Xenopus* melanocytes located on the head and tail for different stages of growth[a]

Stage	Location	Damage Threshold [mJ/cm^2] (N = 2, M = 5)	Average Depth of Melanocytes from surface [μm ± SD] (N = 3, M = 5)
35	Head	2.8-3.4	31 ± 8
35	Tail	9.6-13.6	33 ± 8 (58 ± 15)[b]
40	Head	2.8-3.4	27 ± 7
40	Tail	4.8-6.2	42 ± 19
46	Head	2.0-2.8	13 ± 4
46	Tail	2.0-5.4	30 ± 11 (surface) 90 ± 20 (spinal cord)

[a]The lower threshold value corresponds to an observable change in the pigmented tissue such as contraction, expansion, or discoloration. The upper threshold value corresponds to melanocyte ablation. The number of specimens is indicated by *N*, while *M* refers to the number of melanocytes per specimen.
[b]Distance from *Xenopus* midline to surface where partially pigmented cells containing melanin were migrating.

3.2. Laser marking and ablation of melanocytes

Drawing micropatterns on individual melanocytes or on clusters of melanocytes is possible because the laser spot size (~2 μm) is significantly smaller than the average melanocyte size, which ranges between 10 and 50 μm. This enables the marking of specific geometric figures *in vivo* to follow the evolution and migration of the cells. For surface melanocytes, a slight separation of tissue is observed at a fluence of 2.0 mJ/cm^2 while ablation occurs for fluence values in excess of 3.0 mJ/cm^2. In contrast, targeting melanocytes located below the surface first causes the skin to contract (most likely a muscle reflex associated with heating the melanocyte) and then, with increased fluence, to separate (the tissue is broken open by excess heating and cavitation bubbles). Media 1 is a short video illustrating contraction and slight skin separation resulting from targeting a melanocyte just below the surface of the tail, for a fluence of 26 mJ/cm^2 and a 200 ms shutter open time. Lastly, when the central area, the melanocyte cell body, is targeted, the melanocyte tends to break into many fragments, which in many cases leads to cavitation bubbles that persist beyond laser pulse delivery.

Figure 3 shows some examples of different ways to mark melanocytes. Spot-like ablation was achieved for melanocytes located on the anterior dorsal side of a stage 46 tadpole (Fig. 3a). Tagging of individual melanocytes with triangles is shown in Fig. 3b, and line patterning in a particularly dark tadpole is shown in Fig. 3c. On average the line patterns were observed to last up to 8 hours before becoming unrecognizable. In addition to these simple patterns, we were able to laser write grids, spirals, and preset designs (not shown here). The ability of the

#148794 - $15.00 USD Received 7 Jun 2011; revised 24 Jul 2011; accepted 24 Jul 2011; published 27 Jul 2011

laser to eliminate a melanocyte was also tested. Figure 3d shows a melanocyte located on the dorsal fin before and after laser irradiation, and then after the application of trypan blue, a biological stain applied to discriminate between live and dead cells, with blue indicating cell death. In these experiments, for spot diameter D, the number of pulses N applied to an area $\pi(D/2)^2$ is given by $N = Rt$ for the stationary sample, and $N = RD/\upsilon$ for the moving sample, where R is the repetition rate, t is shutter duration, and υ is that scan speed [25]. Thus, for a laser fluence F, the dosage is NF. For the four images in Fig. 3, the dosages were: (a) 2 M mJ/cm^2, (b) 12 M mJ/cm^2, (c) 30 M mJ/cm^2, and (d) 32 M mJ/cm^2. With increased exposure to laser pulses, the melanocyte ablation changes from controlled spot-like ablation (Fig. 3a) to partial fragmentation (Fig. 3b), then to noticeable cavitation bubbles (Fig. 3c), and finally to collateral tissue damage (Fig. 3d). For labeling and drawing patterns on melanocytes, it is best to avoid bubble formation; therefore, dosages should be between 2 and 10 M mJ/cm^2.

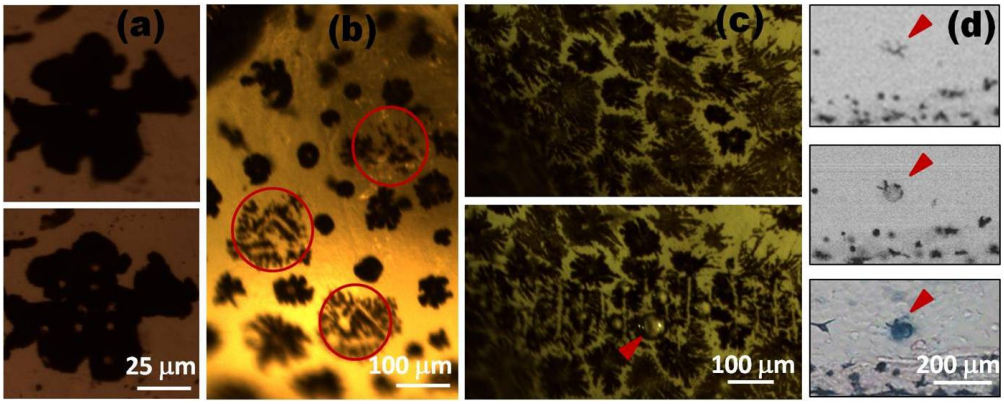

Fig. 3. Different methods to mark melanocytes. (**a**) Top image is a melanocyte located on anterior dorsal side of a stage 46 *Xenopus* before laser ablation and the bottom image shows multiple ablated spots after a laser fluence of 2 mJ/cm^2 and a shutter duration of 10 ms. (**b**) Tagging of individual melanocytes located near the tadpole's eye with triangles using a fluence of 2 mJ/cm^2 and scan speed of 50 μm/s. (**c**) Before and after images of lines drawn on a dark wild-type stage 36 *Xenopus* for a 14 mJ/cm^2 fluence and 150 μm/s scan speed. The red marker points to a long-lasting cavitation bubble. (**d**) Top image of melanocyte located on dorsal fin before laser ablation, middle image is the melanocyte after laser irradiation at 26 mJ/cm^2 and shutter duration of 200 ms, and the bottom image shows a dark blue coloring of the ablated area, after bathing the *Xenopus* in the vital stain trypan blue, which indicates cell death.

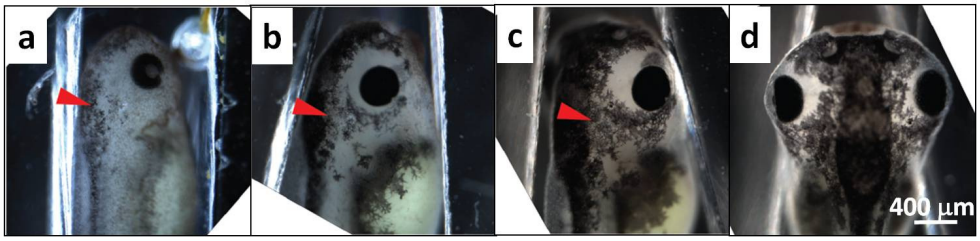

Fig. 4. Images of melanocyte migration after clearing a large area of melanocytes using laser ablation (raster scan with line spacing of 5 μm, F = 6 mJ/cm^2, scan speed = 150 μm/s). Red arrowheads indicate the position of ablation (**a**), 19 hrs later (**b**), and 28 hrs later (**c**). (**d**) shows a dorsal image comparing the left (nonablated) and right (ablated) side of the *Xenopus* 28 hrs after laser ablation.

Although no visible scarring from tagging or line patterning of surface melanocytes was observed, we needed to determine if the laser ablation would somehow inhibit melanocyte migration and/or regeneration. Therefore, preliminary investigations were carried out by recording time-lapse videos of stage 35 *Xenopus* tadpoles with a 150 μm x 200 μm area ablated from the anterior dorsal region, as illustrated in Fig. 4. The images indicate that after

#148794 - $15.00 USD Received 7 Jun 2011; revised 24 Jul 2011; accepted 24 Jul 2011; published 27 Jul 2011

28 hrs new melanocytes move into the ablated area. We also found that when surface cavitation bubbles did form, the skin shed and new melanocytes filled the regions (Media 2).

3.3. Targeting melanocytes to create collateral damage

Laser ablation of melanocytes can also be used as a technique to locally disrupt other tissue, which is of importance for loss-of-function studies in developmental biology. To illustrate this use of the laser, we studied the regeneration process in the *Xenopus* tadpole tail. If the tail of a stage 40 *Xenopus* is amputated with a scalpel, the missing part will regenerate [26,27]. It has further been shown that complete surgical extraction of the spinal cord after tail amputation causes the remaining tail to regenerate abnormally [28]. We used laser ablation to study the influence of localized spinal cord damage (rather than complete spinal cord excision) on tail regeneration, using absorption by melanocytes near the spinal cord to cause targeted insults to the spinal cord itself.

Targeting melanocytes (highlighted in Fig. 5a) with laser powers in excess of the ablation threshold allowed damage to surrounding tissue within a spherical region of diameter, on average, 35 μm. Histological sections showed that the spinal cord and portions of the dorsal muscles were damaged in this targeted region (Fig. 2d). Unlike damage above or below the spinal cord, which had no effect on the tail regeneration, damage to the spinal cord, even far from the amputation plane, caused a sharp deviation in shape of the regenerated tail, (compare Fig. 5c and 5d). Moreover, distinct differences in the regenerated tail were observed when targeting different positions or more than one position of the spinal cord. For example, targeted insults close to the amputation plane typically caused the regenerate to bend in the dorsal direction, whereas insults further anterior caused more complex shape changes. The results of these regeneration experiments are described in detail in [29].

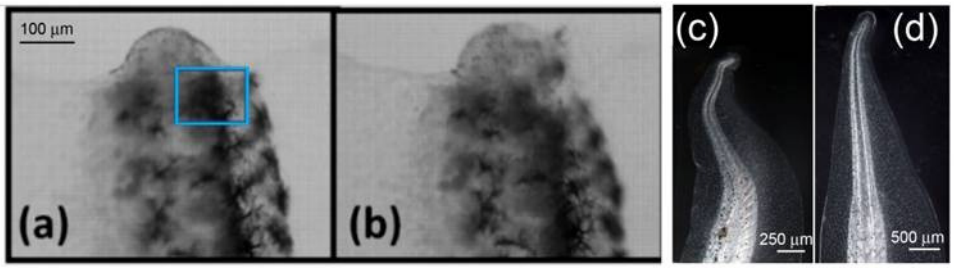

Fig. 5. Tail regeneration after targeting the spinal cord. (**a**) Image of the position where the tail was amputated from a stage 40 *Xenopus* tadpole. The blue box highlights the region targeted by the laser. (**b**) Image after targeting laser in 10 locations inside blue box with laser fluence of 26 mJ/cm^2 and a 200 ms shutter duration. The dark melanocytes that were targeted are gone. (**c**) An image showing the same tail after 1 week. (**d**) The normal shape of a regenerated tail.

4. Discussion

Although the exact ablation mechanism is yet to be determined, we can elucidate its nature based on our observations and previous theoretical and experimental studies [1,30]. At low fluences, ablation is a result of free-electron-induced chemical decomposition (bond breaking) of biomolecules, while at higher fluences, cumulative thermal heating plays a role and long-lasting cavitation bubbles can be observed. These bubbles are related to molecules in the tissue dissociating into volatile fragments, and can cause dislocations to the surrounding tissue. In addition to the fluence, the concentration of melanin in cells also determines the mechanism of ablation by changing the effective absorption coefficient.

Patterning individual melanocytes is a useful technique for following migration of specific cells or clusters of cells, whereas ablation of single or multiple melanocytes lends itself well to the study of melanocyte regeneration and wound healing abilities. By monitoring time-lapse videos of a patch of melanocytes cleared by laser ablation, we observed melanocytes filling the cleared area (Fig. 4). We believe not only that this method is useful for studying

#148794 - $15.00 USD Received 7 Jun 2011; revised 24 Jul 2011; accepted 24 Jul 2011; published 27 Jul 2011

regenerative and migratory melanocyte properties, but also that it makes possible *in vivo* scratch test studies. Presently scratch tests are performed *in vitro* by removing a region of confluent cells grown in a Petri dish and monitoring its repopulation [31]. Moreover, the ability to clear patches of densely spaced melanocytes is of great interest because melanocytes normally exhibit contact inhibition, but can be induced to display cancer-like behaviors; thus, this technique can be used for controlled *in vivo* studies of neoplastic behaviors [17].

The localized, *in vivo* loss-of-function experiments made possible by laser ablation of melanocytes also show promise, as demonstrated by the application to tail regeneration. Targeting specific regions of the spinal cord allows for systematic exploration of the short- and long-distance signaling mechanisms affecting the shape of the regenerated tail—details inaccessible with classic excision experiments [28]. The method can also be extended to areas devoid of melanocytes by staining relevant target cells [30].

5. Conclusion

We have demonstrated the use of an ultrafast Ti:sapphire oscillator for an array of ablation experiments on *Xenopus laevis* tadpoles with specific focus on studies in developmental biology. Typical laser ablation thresholds for different ages (and corresponding developmental stages) of *Xenopus* tadpoles are measured to provide a reference for different modalities of marking and ablation of melanocytes. The ability to label and draw patterns on melanocytes is useful for studies on melanocyte regeneration and migration. Moreover, fs-lasers can be used to clear patches of melanocytes for *in vivo* scratch assays and cancer studies. Lastly, the method can be used for loss-of-function experiments by targeting selected regions of melanocytes, demonstrated here by showing disruptive changes in tail regeneration as a consequence of targeted spinal cord ablation. This combined ability to tag, draw patterns, and ablate melanocytes makes the ultrafast laser a compelling tool for exploring developmental biology mechanisms in *Xenopus* and similar organisms.

Acknowledgments

DSA was supported by NIH 1K22-DE016633. ML gratefully acknowledges funding support of NIH grant GM078484, and of the Telemedicine and Advanced Technology Research Center (TATRC) at the U.S. Army Medical Research and Materiel Command (USAMRMC) through award W81XWH-10-2-0058. FGO thankfully acknowledges the LEEG program at Los Alamos National Laboratory.

#148794 - $15.00 USD Received 7 Jun 2011; revised 24 Jul 2011; accepted 24 Jul 2011; published 27 Jul 2011